Thermochimica Acta, 196 (1992) 213–220
Elsevier Science Publishers B.V., Amsterdam

Study of the phase diagram water fraction of the system water–glycine–sucrose by DTA and X-ray diffraction methods

E.Ju. Shalaev [a], D.V. Malakhov [b], A.N. Kanev [a], V.I. Kosyakov [b],
F.V. Tuzikov [a], N.A. Varaksin [a] and V.I. Vavilin [a]

[a] *NPO "Vector", 633159 Novosibirsk Region, Koltsovo (USSR)*
[b] *Institute of Inorganic Chemistry of the Siberian Branch of the Academy of Sciences of the USSR, Prospekt Akademika Lavrentieva 3, 630090 Novosibirsk (USSR)*

(Received 17 April 1991)

Abstract

The system water–glycine–sucrose was studied at temperatures below 0 °C by DTA and X-ray diffraction methods. The hexagonal ice and β-glycine formations were detected, but other crystal phases were not. Eight isopleths crossing the angles of water and glycine were studied. The water fraction of the plane phase diagram, involving a monovariant line of the secondary crystallization water + glycine and eight isotherms, was plotted.

INTRODUCTION

Information about the phase diagrams of the aqueous systems containing polyols, carbohydrates and aminoacids is used in cryobiology and biotechnology [1,2]. A feature of these systems is their tendency to form a glassy state, which stimulates their protective action towards the freezing and freeze-drying of different biological objects [3]. The equilibrium phase diagrams of such systems are poorly investigated. The goal of the present paper is to study the phase diagram water fraction of the system water–glycine–sucrose. The components of this system are used for protection of biological materials during freezing and freeze-drying.

EXPERIMENTAL

The glycine and sucrose (Serva, analytical grade) were dried to constant mass at 70 °C under vacuum. Solutions were prepared using bidistilled water. All concentrations of solutions are expressed as percentage by mass. The error of composition determination, evaluated from the weighing error and reagent purity, was ±0.05%. The studied compositions belong to eight vertical isopleth sections (Fig. 1).

0040-6031/92/$05.00

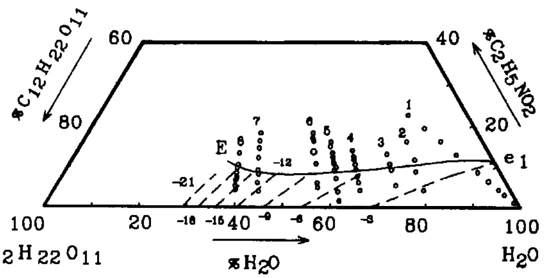

Fig. 1. The water part of the plane phase diagram of the system H_2O–$C_2H_5O_2N$–$C_{12}H_{22}O_{11}$ involving eight isotherms: the studied compositions; e_1E: the projection of the line of the secondary crystallization $H_2O + C_2H_5O_2N$. Dotted lines are isotherms.

The phase transition temperatures were measured by location of the peaks on DTA curves. Silica ampoules (3 mm inside diameter) located in a brass block were used as holders for the sample and a reference (silica). The sample volume was 30 μl. The combined chromel–alumel thermocouples were calibrated over the range from −100 °C to 0 °C using a standard platinum resistance thermometer as well as by the melting points of ice (0 °C), mercury (−38.87 °C) and cyclohexane (melting point +6.5 °C; temperature of S–S transition −87 °C) [4]. Cooling was performed to −120 to −150 °C at the rate of 20–30 K min^{-1}. The heating rate was 2.7 ± 0.05 K min^{-1}. The temperature measurement error was 0.5 °C.

The phase composition of the samples was established using X-ray powder diffraction on a Dron UM1 diffractometer (wavelength of Co Kα radiation $\lambda = 1.79$ Å) and data from refs. 5 and 6.

RESULTS AND DISCUSSION

Binary systems

Water and glycine ($C_2H_5O_2N$) form a eutectic system. The eutectic temperature is -3.6 ± 0.1 °C; the composition is 11.34 ± 0.1 mass% of $C_2H_5O_2N$ [7]. The data from X-ray analysis carried out by us showed that the eutectic involves hexagonal ice and β-$C_2H_5O_2N$. Other phases were not detected.

The system H_2O–$C_{12}H_{22}O_{11}$ (sucrose) appears to be eutectic and has incongruently melting hydrates [8]. However, water alone is crystallized by freezing–annealing the water-rich compositions. The eutectic crystallization failed. The water liquidus extends beyond the eutectic point, the coordinates of which are evaluated by the intersection of the left and right monovariant lines of phase equilibria [9].

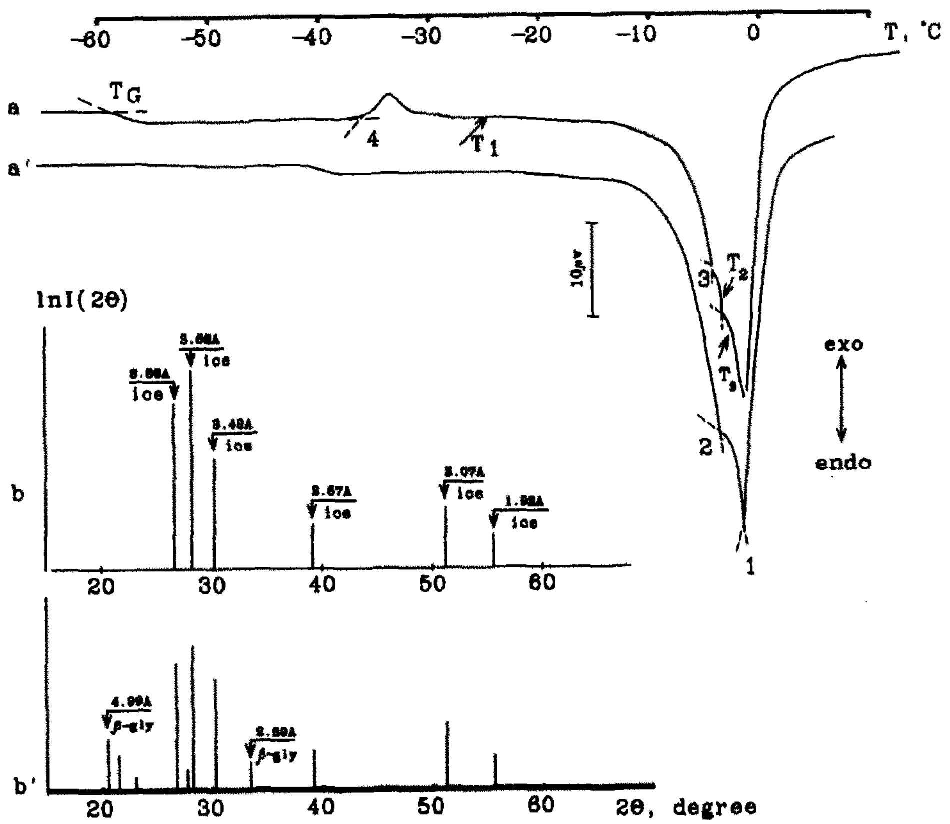

Fig. 2. Curves of DTA (a, a′) and X-ray diffraction diagrams (b, b′) of a specimen consisting of 6.4% $C_2H_5O_2N$ and 3.6% $C_{12}H_{22}O_{11}$; (a′, b′) after annealing at T_3.

The system H_2O–$C_2H_5O_2N$–$C_{12}H_{22}O_{11}$

There is no information on the phase diagram of the present system in the literature. It may be noted that phase transitions involving sucrose or its hydrates were not observed for either the ternary system or the H_2O–$C_{12}H_{22}O_{11}$ system. Also, the second crystallization of $H_2O + C_2H_5O_2N$ is hindered for compositions with an elevated content of $C_{12}H_{22}O_{11}$. This factor rules out the use of known methods of investigation of phase diagrams of the ternary system based on DTA data to allow the volume of experiments to be reduced [10].

Figure 2 gives DTA curves and X-ray diagrams of one of the compositions as an example. There are only ice lines on the X-ray diagrams. The DTA curve represents one exothermic peak, three poorly resolved endothermic peaks and an endothermic stage. Annealing at T_1 leads to disappearance of the exothermic peak and occurence of lines of β-glycine on the X-ray diagram. On annealing at T_2, only the peaks 1 and 2 are left

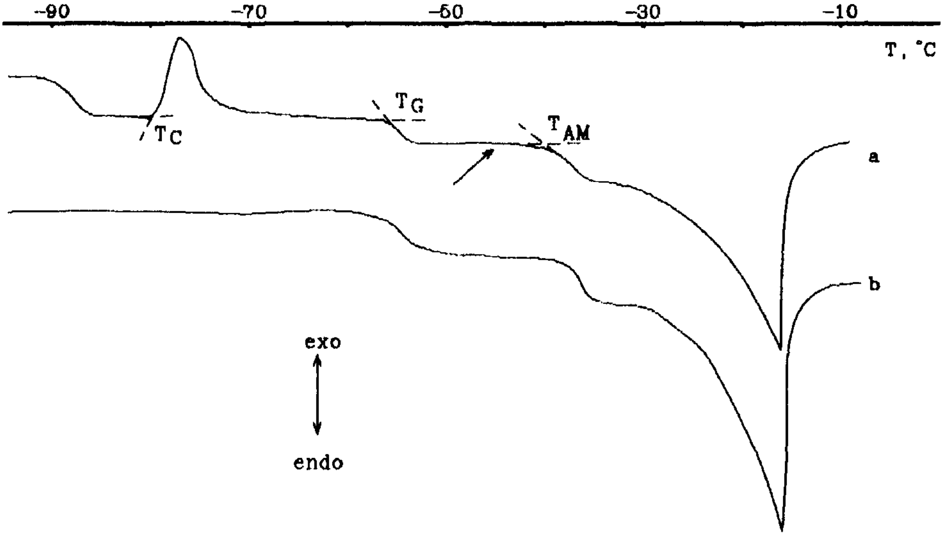

Fig. 3. DTA curves of a specimen consisting of 5.73% $C_2H_5O_2N$ and 57.02% $C_{12}H_{22}O_{11}$; (b) after annealing.

on the DTA curve. As a result of annealing at T_3 the four features are observed again. Also, the temperatures of transitions 3 and 4 are decreased by decreasing the heating rate; the positions of peaks 1 and 2 are not affected. Thus, the exothermic effect is due to the secondary crystallization $H_2O + C_2H_5O_2N$. Transition 3 is likely not to be an equilibrium; so far its identification has not been achieved. The peaks 2 and 1 may be assigned to the melting of $\langle H_2O\rangle + \langle C_2H_5O_2N\rangle$ (a surface of the secondary crystallization $H_2O + C_2H_5O_2N$) and $\langle H_2O\rangle$ (liquidus of water) respectively. As with the system H_2O–$C_{12}H_{22}O_{11}$, eutectic melting is not observed. The endothermic stage is probably attributable to the glass transition of the liquid remaining after the primary and secondary crystallizations.

The DTA curve of one of the concentrated solutions is shown in Fig. 3 (3b—after annealing). The endothermic peak is connected with melting ice, according to the X-ray diagram. The two endothermic stages T_G and T_{AM} (glass transition and premelting transition of unknown nature) and the exothermic peak T_C (water crystallization) are observed also for concentrated binary solutions of water–sucrose [11]. The results given in the present work are true for the transition whose equilibrium nature is confirmed by annealing and X-ray diffraction analysis. Equilibrium transitions as observed for other investigated compositions are thus due to the melting of either $\langle H_2O\rangle$ or $\langle H_2O\rangle + \langle C_2H_5O_2N\rangle$.

The general form of isopleths for $(X_s/X_w) = R =$ const. (where X_s and X_w are mass fractions of sucrose and water) is shown in Fig. 4. Here, ne′ and me′ are the intersection lines of the profile plane with a line surface of

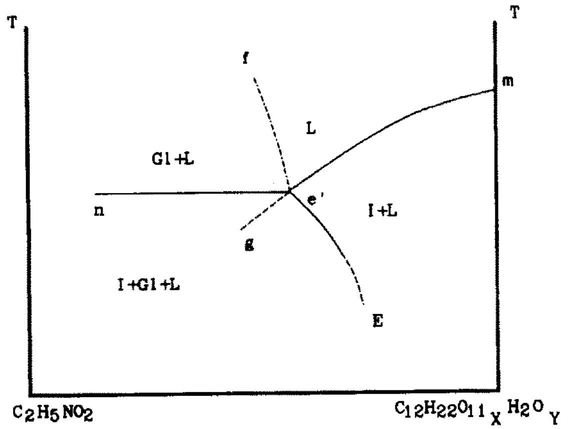

Fig. 4. The general appearance of isopleths 2–8 (Fig. 1): $X = 0.192$; 0.249; 0.330; 0.379; 0.424; 0.556; 0.603; $Y = 1 - X$.

the secondary crystallization $H_2O + C_2H_5O_2N$ (parallel to the plane of composition) and the water liquidus surface. These lines have a common point of intersection, e′. The line e′E corresponds to the surface of the secondary crystallization located in the water crystallization volume. The transitions connected with this line (the equilibrium $\langle H_2O \rangle$ + solution–$\langle H_2O \rangle + \langle \beta\text{-}C_2H_5O_2N \rangle$ + solution) are observed only for section 2 (Fig 1). As for the remaining compositions located on the volume of water, the secondary crystallization $H_2O + C_2H_5O_2N$ does not occur.

Tables of experimental points belonging to the surfaces L/I + L and L + Gl/L + Gl + I (L = solution, I = ice, Gl = glycine) were compiled from the DTA data. To use the tabular data it is necessary to determine a law of interpolation between the table sets, namely, to define an analytical description of these surfaces. This description will make it possible to represent the obtained data set in a compact form and to determine the phase transition temperatures for samples having an arbitrary composition. Also, the combined treatment of the data permits random undershoots to be rejected and the experimental results to be smoothed. In the present study a polynomial description of phase equilibrium surfaces is selected. Certainly there are no physicochemical reasons in favour of just this model, yet a variety of circumstances makes it possible to predict the acceptability of our choice. Firstly, the surfaces are smooth; secondly, the obtained polynomials are not intended for a distant extrapolation; thirdly, and lastly, the coefficients of the polynomials have no physical meaning.

For the water liquidus surface the coordinates of $M = 272$ points are determined by experiment

$$x_{2i},\ \Delta x_{2i},\ x_{3i},\ \Delta x_{3i},\ T_i,\ \Delta T_i;\quad i = 1, \ldots, M \tag{1}$$

where x_{2i} and x_{3i} are mass percentages of glycine and sucrose at the ith point, respectively; T_i is the measured temperature (in °C) at this point; and Δy denotes the evaluation of a standard root-mean-square deviation of the value "y". All the measurements are considered to be individual, i.e. there are some points of the same composition but various temperatures in set (1); averaging of these latter ones and recalculation of their errors are not carried out. The use of the χ^2 criterion has made it possible to accept the hypothesis of a normal law of error distribution and to formulate the following least-squares problem

$$\sum_{i=1}^{N} \omega_i [P(x_{2i}, x_{3i}) - T_i] \to \min \tag{2}$$

where ω_i is a statistical weight of the ith point

$$P(x_{2i}, x_{3i}) = \sum a_j f_{\mathrm{NUM}(j)}(x_{2i}, x_{3i})$$

where N is the number of the used base functions a_j, $j = 1, \ldots, N$ are the evaluated parameters, and $f_{\mathrm{NUM}(j)}(x_{2i}, x_{3i})$ is a corresponding base function from the table containing Nx_2 lines.

$$\begin{array}{llll}
1 & x_2 & x_3 & \ldots \\
x_2 & x_2x_3 & x_2x_3^2 & \ldots \\
x_2^2 & x_2^2x_3 & x_2^2x_3^2 & \\
\cdot & & & \\
\cdot & & & \\
x_2^{Nx_2-1} & x_2^{Nx_2-1}x_3 & x_2^{Nx_2-1}x_3^2 &
\end{array}$$

Equation (2) was solved using a singular decomposition [12] of a fundamental matrix which allowed the risk of poor conditionality [13] to be avoided.

The correct selection of statistical weights is a rather delicate matter, in that it is essential to take account of the error resulting from, not only the temperature determination, but also the compositonal analysis. To realize this requirement the method of integrated statistical weights [14] was used.

To check the quality of the description, the following stastistics were calculated and compared with tabular ones [15]: the sum of squares of weighted residuals, the validity variance, the coefficient of asymmetry and the excess characteristic. The difference between the experimental and calculated values of temperatures was evaluated for each point of a scheme. When the difference exceeded the trebled (30 rule) error in T, taking into account the confluent additives, then the corresponding point was eliminated from the scheme. There were eight points of this type, but after their elimination and a recalculation their effect was absent. The manner of distribution of signs of residuals makes it possible with certainty to state the nonoccurrence of trends. The number of conditionality [12] proved to be 1.43×10^{10}, which is perfectly acceptable in calculations of double precision.

It is essential to note that the definiteness of a Gesse matrix was analysed for each point of the scheme; in no case was it positively definite, i.e. the surface was not concave.

Thus, a surface description unencumbered by oscillation characteristic of the polynomial approximation was obtained.

A result of our calculations is the following expression describing the water liquidus surface in the system water–glycine–sucrose.

$$\begin{aligned} T_1 = & -0.246365x_2 - 6.15447 \times 10^{-3}x_2^2 + 1.05526 \times 10^{-2}x_3 \\ & - 8.52571 \times 10^{-3}x_3^2 + 2.98789 \times 10^{-4}x_3^3 - 4.85447 \times 10^{-6}x_3^4 \\ & + 2.08168 \times 10^{-8}x_3^5 - 1.76408 \times 10^{-4}x_2x_3^2 + 1.29391 \times 10^{-10}x_2^2x_3^3 \\ & + 6.73101 \times 10^{-7}x_2^2x_3^4 - 2.05364 \times 10^{-8}x_2^2x_3^5 \end{aligned} \quad (3)$$

For the secondary crystallization water + glycine surface, the coordinates of 101 points were determined. The surface of secondary crystallization is linear [16], hence it follows that for the compositions located in the $C_2H_5O_2N$ volume (to the higher side of the line e_1E in Fig. 1) the temperature T_2 of the secondary crystallization is determined by the $X_s/X_w = R$ ratio and is independent of the $C_2H_5O_2N$ content. The t_2 dependence is described by the polynomial

$$T_2 = 3.6 - 3.984280R - 3.711138R^2 \quad (4)$$

The projection of the secondary crystallization line e_1E and isotherms at eight temperatures, as based upon expressions (3) and (4), are shown in Fig. 1.

The studied water angle of the phase diagram of the system H_2O–$C_2H_5O_2N$–$C_{12}H_{22}O_{11}$ makes it possible to define an order of crystallization of the solution components, a sample phase composition at the chosen temperature, as well as a curve shape of the secondary crystallization $\langle H_2O \rangle + \langle C_2H_5O_2N \rangle$ in the isopleths crossing the water peak. (Such profiles make possible the representation of the sample phase-composition changes in the course of freeze-drying). This information, supplemented by data on metastable states, is needed to develop a scientifically based technology for freeze-drying of biological materials.

REFERENCES

1 F. Franks The properties of aqueous solutions at subzero temperatures, in F. Franks (Ed.) Water—A Comprehensive Treatise, Vol. 7, Plenum Press, New York 1982.

2 F.H. Cooks and W.F. Brower, Cryobiology, 11 (1974) 340.

3 P.Boutron, P. Mehl, A Kaufman and P. Angibaud, Cryobiology, 23 (1986) 453.

4 J. Šesták, Thermophysical Properties of Solids. Their Measurements and Theoretical Thermal Analysis, Academia, Prague, 1984.

5 M. Blackman and N.D. Lisgarten, Proc. R. Soc. London, Ser. A, A239 (1957) 93.

6 A.I. Kitaygorodsky, The Structure of Organic Substances, Nauka, Moscow, 1980 (in Russian).

7 A.N. Kanev, V.I. Kosyakov, D.V. Malakhov and E.Yu. Shalaev, Izv. Sib. Otd. Akad. Nauk SSSR, Ser. Khim. Nauk, 3 (1989).

8 F.E. Young and F.T. Jones, J. Phys. Colloid. Chem., 53 (1949) 1334.

9 A.N. Kanev, V.I. Kosyakov, D.V. Malakhov and E.Yu. Shalaev, Izv. Sib. Otd. Akad. Nauk SSSR, Ser. Khim. Nauk, (2) (1989) 11.

10 D.A. Petrov, Zh. Fiz. Khim., 14 (1940) 1498.

11 B. Luyet and D. Rasmussen, Biodynamica, 10 (1968) 167.

12 J.H. Wilkinson and C. Reinsch, Handbook for Automatic Computation, Vol. II. Linear Algebra, Springer-Verlag, Heidelberg.

13 A.N. Tikhonov and V.Ya. Arsenin Methods of Solution of Incorrect Problems, Nauka, Moscow, 1986, 288 pp. (in Russian).

14 V.V. Phedorov, Theory of Optimum Experiment, Nauka, Moscow, 1971, 312 pp. (in Russian).

15 L.N. Bolshev and N.V. Smirnov, Tables of Mathematical Statistics, Nauka, Moscow, 1983, 416 pp.

16 Y.Ja. Anosov, M.I. Ozerova and Yu.A. Fialkov, The Bases of Physico-chemical Analysis, Nauka, Moscow, 1976, 504 pp. (in Russian).